Wave-packet theory of coherent carrier dynamics in a semiconductor superlattice

Mark L. Biermann* and C. R. Stroud, Jr.
The Institute of Optics, The University of Rochester, Rochester, New York 14627
(Received 29 June 1992; revised manuscript received 19 October 1992)

An investigation of coherent carrier dynamics in optically excited, semiconductor superlattices is presented. A $\mathbf{k}\cdot\mathbf{p}$, local pseudopotential method is used for the band-structure calculation. The coherent dynamics are described in a wave-packet formalism similar to that applied in atomic systems. The method is then applied to specific quantum-well and superlattice systems. The results of the formalism in these examples are consistent with experimental studies in similar systems. Coherent dynamics analogous to those seen in atomic systems are predicted in semiconductor systems. These phenomena include the decay and revival of the wave packet.

I. INTRODUCTION

When a short laser pulse excites a quantum system, a spatially localized wave packet is formed. This phenomenon has been observed in both atomic and molecular systems.[1] Theoretical formalisms have been described for modeling this type of wave-packet phenomena in these systems.[2] In this paper, we describe a theoretical model of wave-packet dynamics in semiconductor-superlattice systems. Interesting predictions of this formalism are also presented.

This theory is of particular interest when considered in light of recent experimental results in semiconductor quantum-well and superlattice systems. These results include the observation of quantum beats in quantum-well systems. In one case, the observed quantum beats were due to the interference between two heavy-hole excitons in a quantum well.[3] Quantum beats can be treated as a special case of the general wave-packet theory described here.[4] In another experiment, an optical pump was used to establish a coherence between a heavy-hole exciton state and a light-hole exciton state within two coupled quantum wells.[5] The interference between these states led to a beat, or modulation, on the diffracted signal in a degenerate four-wave mixing experiment. Additionally, wave packets have been observed experimentally in a GaAs, $Al_{0.35}Ga_{0.65}As$ double-quantum-well structure.[6] These wave packets arise due to the interference between two superlattice states. Striking evidence of the existence of wave packets in a coupled-quantum-well system has been provided by the observation of coherent submillimeter-wave emissions when such a system was excited by a short laser pulse.[7] These emission are the direct result of the oscillation of the carrier wave packet between the coupled, quantum wells and the resulting induced dipole. The frequency of the submillimeter-wave emissions follows directly from the energy spacing of the two eigenstates coherently excited by the short optical pulse. Finally, a large, triply resonant, third-order nonlinear susceptibility has been observed in a quantum-well system in which the eigenstates of interest are approximately equally spaced in energy.[8] This result agrees on a qualitative level with the predictions of the theory described here.

The paper is organized as follows. In Sec. II a general description of the wave-packet theory is given. This description includes brief accounts of the band-structure theory employed and the methods used in accounting for effects such as excitons. Incoherent processes leading to the destruction of the wave packet are also briefly discussed. In Sec. III this theory is applied to a two-subband wave packet in a single quantum well. In Sec. IV the significance of using subbands that are not equally spaced in energy in the formation of wave packets is explored. This is done using both a three-subband wave packet and a five-subband wave packet. Finally, comparisons are made between these theoretical results and the result of various experiments and conclusions are drawn in Sec. V.

II. GENERAL THEORY

The theory we use to model wave packets in semiconductor-superlattice systems has a number of important features. First, it accounts for the nature of the bulk materials used in fabricating superlattices. The symmetry characteristics of the bulk materials and of the superlattice are used so that proper subband bending and subband anticrossings are obtained. Additionally, the theory can be used to properly describe superlattice and quantum-well systems that are fabricated using an arbitrary number of bulk-material layers in the heterostructure cycle. It is worth noting that the formalism brings together techniques from solid-state and atomic physics. Band-structure calculation methods developed using solid-state theory are used to provide the superlattice subband energy positions and envelope functions. Techniques developed to describe wave-packet phenomena in Rydberg atomic systems are used to describe the coherent dynamics the semiconductor-superlattice wave packets display.[9]

The superlattice band-structure calculation technique is based on a $\mathbf{k}\cdot\mathbf{p}$ perturbation method of Smith and Mailhiot.[10] The method is critical in the present discus-

sion since the form of the wave functions of the allowed electron states in the solid follows naturally when the technique is applied. The wave functions are required to calculate momentum matrix elements and other quantities needed in optical studies of solids. This formalism is unique in that it combines the $\mathbf{k}\cdot\mathbf{p}$ perturbation method with a local pseudopotential method to find the bulk-material eigenfunctions. This allows one to properly account for symmetry considerations and bulk-material-specific characteristics throughout the superlattice band-structure calculation.

The formalism can be broken down into four distinct steps. The first is the use of an empirical-local-pseudopotential method to find the zone-center basis functions for the constituent bulk materials used in the superlattice. The next step is to use Löwdin perturbation theory[11] with the $\mathbf{k}\cdot\mathbf{p}$ operator to find the bulk-material band structure for each of the constituent materials used in the superlattice. The Hamiltonian used in the perturbation expansion for material i is

$$H_i = H_R + \Delta V^i + H^i_{\text{s.o.}} + H^i_{\text{st}} , \tag{1}$$

where

$$\Delta V^i = V^i - \frac{1}{n}(V^a + V^b + \cdots + V^n) \tag{2}$$

and

$$H_R = \frac{p^2}{2m} + \frac{1}{n}[V^a(r) + V^b(r) + \cdots + V^n(r)] , \tag{3}$$

where ΔV^i is the difference between the pseudopotential of material i and the average pseudopotential of all constituent materials and H_R is the reference Hamiltonian, defined for convenience. Also, $H^i_{\text{s.o.}}$ arises from the spin-orbit interaction and H^i_{st} is due to the stress interaction, resulting from lattice mismatch, in material i. Treating the Hamiltonian in this way allows one to account explicitly for the various physical phenomena affecting the bulk materials.

In the third step, the bulk-material eigenfunctions of the constituent materials, both the Bloch and evanescent states, are matched at the interfaces in the superlattice using the normal component of the current density operator. This allows one to establish matching conditions which dictate how the bulk eigenstates mix to form the superlattice eigenstates. It is worth mentioning that the energy alignment between the constituent materials is based on empirical results. That is, the valence-band offset between the different materials is obtained from experiment.[12] In the fourth and final step, translational symmetry of the superlattice is used to find an eigenvalue equation for the wave vectors and eigenfunctions of the superlattice. This eigenvalue equation typically uses matrices of small dimensionality, that is, matrices of size between 4×4 and 12×12. This adds to the appeal of this method. The results for the energy levels and envelope functions of the superlattice eigenstates are then used in the wave-packet formalism.

It should be noted that the paper of Smith and Mailhiot which outlines this approach concentrates on a two-material-layer-repeat-cycle superlattice.[10] The questions which arise when dealing with a superlattice with an arbitrary number of materials in a superlattice repeat cycle are addressed in a short appendix. The flexibility gained by fully developing the implementation of a formalism which can deal with an arbitrary of material layers is crucial to the overall theory described here. This is because one would like to be able to describe systems than a single, square quantum well. Two coupled wells, for instance, can be described using a four-material-layer-repeat-cycle superlattice. These extensions were implemented in developing the present model of superlattice wave packets. These enhancements to the theory include techniques for treating applied electric fields, applied and internal strains, and other phenomena that are dependent upon the particular form of the superlattice. These are not discussed in detail here.[5] This theory has been applied to coupled-well systems for the purpose of modeling the effect of strong coupling on the energy levels of quantum wells.[13]

The results of the superlattice band-structure calculation can now be applied in modeling the coherent dynamics of semiconductor-superlattice wave packets. The wave-packet model is based on techniques developed for the purpose of describing wave packets in Rydberg atoms.[14,15] Wave-packet models have been developed for radially localized atomic wave packets,[9] angularly localized wave packets,[16] and three-dimensionally localized atomic wave packets.[2] All atomic wave-packet models and the semiconductor-superlattice wave-packet model have a number of features in common. For example, all models assume a laser excitation pulse of time length much less than the phase relaxation time for the system, T_2. This allows for the observation of the coherent dynamics. The model used to describe wave packets in a semiconductor superlattice most closely parallels that used for the radially localized atomic case. This follows from the fact that both the radially localized atomic wave packets and semiconductor-superlattice wave packets arise when several eigenstates of different energies are simultaneously excited using a short laser pulse. The angular momentum of all the eigenstates combined in both of these wave-packet types is the same.

All information about the superlattice wave-packet, or superposition, state is contained within the wave function. The wave packet can be expressed in the general form

$$\Psi(t) = \sum_n e^{-i\omega_n t} C_n \psi_n , \tag{4}$$

where C_n is an amplitude coefficient that describes the initial contribution of the superlattice state n, ψ_n is the envelope function of the superlattice state, ω_n is the frequency of the subband state, and n runs over the states included in the wave packet. The frequency is given by $E_n = \hbar\omega_n$ where E_n is the energy of the subband measured from the bulk conduction-band edge for an electron state and from the bulk valence-band edge for a valence state. The subband envelope functions and eigenenergies are provided by the band-structure calculation formalism. It is seen that the coherent time dependence of the

wave packet depends strongly on the subband energy separations. Since these energy spacings depend directly on the form of the superlattice or quantum-well system used, semiconductor-superlattice systems provide the possibility of tailoring the design of a heterostructure in such a way as to obtain a specifically desired time dependence. For instance, if all the subband eigenstates involved in the wave-packet formation are evenly spaced in energy, a simple harmonic time dependence is obtained in Eq. (4). Hence the wave packet would simply undergo periodic variations until the destruction of the intersubband coherences by incoherent processes.

Great care must be used in choosing which superlattice eigenstates are to be included in a given wave-packet model, that is, which ψ_n's are to be used. In systems such as Rydberg atoms the choice of eigenstates to be used in the wave packet is self-evident. In superlattice systems, the choice is not as obvious. In the wave-packet experiment of Leo *et al.*,[6] the first two electron exciton states were used as the basis states of the wave packet. Such a straightforward choice may not always be possible. This is illustrated in Fig. 1 where an isolated quantum-well system is shown schematically. The light-hole, heavy-hole, and electron states are labeled and two different exciting laser pulses are also included in the illustration. We note first that the hole states are closer together than the electron states, as is generally the case due to the more dispersive nature of the bulk and quantum confined electron states. We next note that the laser pulse that is narrower in frequency bandwidth, that is, the pulse with a narrower energy spread, overlaps only the first electron state in the conduction band and the fist three hole states

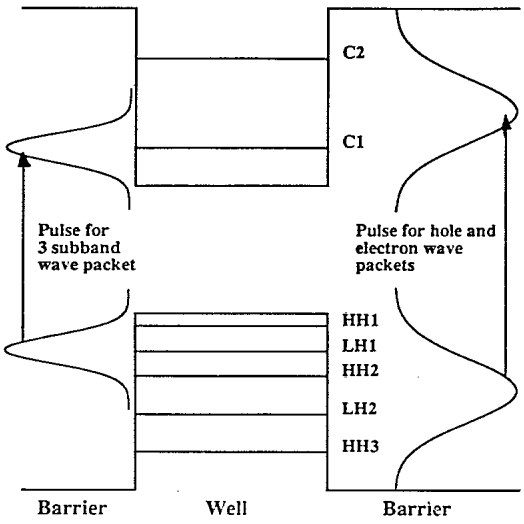

FIG. 1. The excitation of an isolated quantum well by laser pulses is illustrated. The horizontal axis is along the superlattice growth direction while the vertical axis is associated with energy. The width, along the vertical axis, of the schematic laser pulse is proportional to its total energy spread. The combination of electron and hole states coupled by a given laser *pulse* is clearly illustrated by the lineup of the subbands and the laser "pulse shapes."

in the valence band. Hence only the first electron state is coupled to the first three hole states, assuming the matrix elements for all three transitions are nonzero. This situation occurs through a proper choice of the laser frequency and pulse strength. Since three hole states are coupled to a single electron state, the three hole states are used as the basis states for a wave packet, and a hole wave packet is formed. In this case Eq. (4) has the specific form

$$\Psi(t)=e^{-i\omega_{\mathrm{HH1}}t}C_{\mathrm{HH1}}\psi_{\mathrm{HH1}}+e^{-i\omega_{\mathrm{HH2}}t}C_{\mathrm{HH2}}\psi_{\mathrm{HH2}} +e^{-i\omega_{\mathrm{LH1}}t}C_{\mathrm{LH1}}\psi_{\mathrm{LH1}}\ , \tag{5}$$

where the subband labels are self-evident. This wave-packet description is, then, quite straightforward

However, the situation which arises when the wider pulse in frequency bandwidth (Fig. 1) is used is much more complicated. It overlaps the first two conduction-band states and the first five valence-band states. Thus there is the possibility for the formation of both an electron wave packet and a hole wave packet. The form of these wave packets would, of course, depend directly on the intersubband transition rates. Assuming a nonzero transition rate exists between the five valence states and each of the two electron states, there will be contributions to the electron wave packet from each of the five hole states. Hence there would be ten transitions that contribute to the form of the two-subband electron wave packet. Conversely, there would also be ten transitions which contribute to the five-subband hole wave packet. This is considerably more complicated than the three-hole subband wave-packet case, which involved only three transitions. Further complicating the second excitation scenario is the possible interference between the hole and electron wave packets and the extreme experimental difficulties involved in attempting to discern which features of observable, coherent-dynamical phenomena are the result of a particular wave packet. A thorough understanding of the subband energy structure and the excitation scheme is then needed to accurately model any wave-packet system.

The method employed for finding the expansion coefficients C_n used in the wave-packet description of Eq. (4) must also be addressed. These coefficients give the amplitude of the associated eigenstate included in the wave packet after the laser excitation, that is, the contribution of that eigenstate to the total wave packet. The coefficients are taken to be proportional to the square root of the interband transition rates. In this formalism, the transition rate is given by Fermi's "golden rule." The transition rate W can then be written as

$$W=\frac{2\pi}{\hbar}\sum_{f,i}|\langle f|H_I|i\rangle|^2\delta(E_f-E_i+\hbar\omega)\ , \tag{6}$$

where i and f label the initial and final subband states of the transition, with energies E_i and E_f, respectively, $\hbar\omega$ is the energy of a laser photon, and H_I is the interaction Hamiltonian, equivalent to $-e\mathbf{r}\cdot\mathbf{E}$ in the electric dipole approximation. The Kronecker δ function serves to conserve energy in the transition. The momentum of an optical photon is small compared to the crystal momentum

of a Bloch electron or hole and so it is neglected in the transition.[17] This leads to vertical transitions in the superlattice system, where "vertical" refers to the orientation of the standard energy versus crystal momentum plots of band structure.

We cast this transition in a more convenient form by writing the sum over states as an integral over energy. We also assume that the final subband states are of a given spin and have a density of states $N(E)$ over a range of energy E to $E+dE$. Performing this integral and writing the result in terms of the fine structure constant α, the Rydberg energy R_H, and the Bohr radius a_H, we obtain

$$W=\tfrac{16}{3}\pi^2\alpha a_H^2\left[\frac{R_H}{\hbar\omega}\right]\left[\frac{c\epsilon_0}{\varepsilon_\nu}\right]n_\nu\frac{p_{cv}^2}{2m}N(E_f)\ , \tag{7}$$

which is similar to a result of Ridley.[17] In this equation, ε_ν is the permittivity of the semiconductor material, n_ν is the photon number at the transition frequency, and $p_{cv}^2/2m$ is equal to one-quarter of the magnitude of the optical matrix element squared, as defined by

$$\sum_{i'}\frac{2}{m}|\langle n_i|\bar{\mathbf{p}}\cdot\bar{\boldsymbol{\varepsilon}}|n_{i'}\rangle|^2\ , \tag{8}$$

where m is the mass of an electron, not an effective mass, the $|n_i\rangle$ are the zone-center states of the superlattice, and the sum is over degenerate pair of eigenstates. We note that the optical matrix element used in Eq. (7) does not contain the dependence on the polarization of the optical field. In writing Eq. (7) in this form, it is taken that the polarization effects have already been accounted for and appear in the magnitude of the quantity p_{cv}^2.

The density-of-states term $N(E_f)$ is treated in an effective-mass model. The effective-mass results for the zone-center eigenstates follow from the band-structure formalism. Typically, the familiar stair-step density-of-states function, exact only in an infinitely deep, isolated square well, is used.[18] However, we have found that the three-dimensional density-of-states function also works well in many cases. This is because the two-dimensional and three-dimensional density-of-states results are approximately equal at eigenenergies of the system. In many cases, numerical results for W are found to be approximately equal, independent of the density-of-states function used.[5]

In associating the transition rates with the expansion coefficients of Eq. (4) a further simplification can be made within the theory. The form of the wave packet depends on the relative amount of each superlattice eigenstate included in the wave packet, as opposed to depending on the absolute population. This result is analogous to the fact that it is the energy spacings, and not the absolute energy spacing, between the constituent subbands that contribute to the wave-packet coherent dynamics. Since we assume small excited populations, it is convenient to write the transition rate in terms of a proportionality. Only those terms which are subband dependent are kept, and we obtain

$$W_n\propto\frac{I_1(n)}{\hbar\omega_1}\frac{|p_{cv}(n)|^2}{2m}N(E_n)\ , \tag{9}$$

where the photon number n_ν has been expressed in terms of the laser intensity at the transition frequency I_1, and the energy of a single photon at that frequency $\hbar\omega_1$. The subscript and argument n refer to a given transition. We see that the subband-dependent terms for a given system are the photon number, the optical matrix element, and the density of states for the final state.

We describe the coherent dynamics of the system, then, by using Eq. (9) for the transition rates and assuming that the amplitudes, the C_n, are normalized to the amplitude results for one of the constituent subbands in the wave packet. This normalization assumption allows one to treat the proportionality $C_n^2\propto W_n$ as an equality. In some situations this proportionality result may not be sufficient. For example, comparisons to some experimental results could require a more complete treatment. In such situations, the complete transition rate result of Eq. (8) is used. By integrating this transition rate over the total laser pulse used to form the wave packet, the absolute population of the excited subbands in the superposition state could be determined. This integration is over the total time extent of the exciting pulse.

Excitonic effects on the formation of the wave packet are addressed as follows. Excitonic effects lead to two possible descriptions of the interference leading to wave-packet formation. One could describe the wave packets as forming due to the interference between either the coherently excited superlattice eigenstates or between the relevant coherently excited superlattice exciton states. The excitonic description is preferred by Leo *et al.*[6] The formalism presented here, however, describes the wave packets in terms of the interference between the superlattice eigenstates themselves. We note that much physical insight can be gained into the coherent dynamics of optically excited semiconductor superlattice systems by applying the theoretical approach presented here. Additionally, excitonic corrections to the intersubband transition energies are used within the theoretical formalism when relevant. Finally, the effect that the formation of excitons has on the interband transition rates is accounted for. One must multiply the transition rate expressions of Eqs. (8) and (9) by the square of the inverse of the effective Bohr radius of the exciton to obtain the transition rate corrected for excitonic effects. This correction has been shown to been an acceptable measure of the excitonic effect on the oscillator strength in physical, quasi-two-dimensional systems[19] and tends to strongly enhance the transition rate. The correction depends most strongly on the reduced effective mass for the transition.[20] Since the effective masses follow directly from the band-structure calculation, this correction can be applied in a straightforward manner.

The final aspect of the theoretical formalism which is addressed is the treatment of the processes that lead to the loss of coherence between the superlattice subbands and, hence, lead to the destruction of the wave packet. These carrier relaxation processes put an upper limit on the time frame in which coherent dynamics can be ob-

served in semiconductor systems. Carrier relaxation processes fall into two classes, scattering processes and emission processes. Scattering processes include carrier-phonon and carrier-carrier scattering.[21] At high electron densities, carrier-carrier scattering can include energy loss to coupled plasmon-phonon modes in addition to collisions with other holes and electrons.[22] In addition to these homogeneous scattering processes, inhomogeneous scattering mechanisms also exist. An example of these is scattering due to interface roughness.[3,23] Emission processes include polar optical phonon emission within the central, or Γ, valley of the direct gap semiconductor, and zone-edge phonon emission.[22] In studies of bulk and quantum-well semiconductor samples, carrier relaxation times, due to various processes, have been measured at between a few tens of femtoseconds and a few picoseconds.[21–24] In studies directed toward surface roughness scattering, relaxation times on the order of 1.5 ps per monolayer of roughness have been reported.[3]

Coherent processes have been observed in quantum beat and wave-packet experiments over time frames of several picoseconds.[3,6] For example, in a wave-packet experiment in a GaAs, $Al_{0.35}Ga_{0.65}As$ double-quantum-well structure one or two periods of the wave-packet oscillation, with a period of 1.3 ps, were observed. In an experiment in which quantum beats were observed between heavy-hole exciton states split due to surface roughness, a relaxation time constant of about 1.2 ps was observed.[3] In this case, approximately three quantum beats, with a period of 1.33 ps, were observed before the coherence was destroyed. Based on this work with quantum beats, it is seen that phase relaxation processes are primarily responsible for the destruction of the wave packet.[3] In any case, the incoherent processes in semiconductor superlattices occur on very rapid time scales and coherent processes are thus greatly restricted.

The relaxation processes are dealt with phenomenologically in the formalism used here. That is, for comparison to experiment it is assumed that the coherent processes continue only as long as the incoherent dephasing mechanisms allow. The characteristic times for these incoherent dephasing mechanisms are contained in the empirically determined population and phase relaxation time constants, T_1 and T_2. The values of T_1 and T_2 in a given system, that is, the time scale over which the coherence is lost, are taken from experimental results for systems similar to those being modeled. For example, since Leo *et al.*[6] observed coherent wave-packet dynamics for approximately 3 ps in their coupled-well experiments, we apply a similar upper limit in comparing our modeling of coupled-well systems to experiment.

It is worth noting that, although the time constraints are considerable for observing coherent phenomena, they are not such that they exclude extensive experimental studies, provided appropriate care is exercised. Carefully controlling a number of experimental conditions would serve to maximize the values of T_1 and T_2 in a given system. These conditions include working with small excited populations to avoid rapid dephasing due to carrier-carrier scattering and similar mechanisms. Additionally, reducing surface roughness at the heterostructure interfaces would help to minimize incoherent processes such as surface roughness scattering. Such requirements can be met by working at low temperatures, using low-energy laser excitation pulses and by using heterostructures of high quality. Our formalism explicitly assumes that these conditions are being met in that small excited populations are used. Implicitly, our formalism also requires that these conditions be met in that we assume the coherent processes continue long enough to be observed.

We now apply this formalism by modeling several systems that are relevant to experimental results or that show particularly interesting behavior.

III. TWO-SUBBAND WAVE PACKET IN AN ISOLATED QUANTUM WELL

We first model a wave packet in an isolated quantum well. The quantum well is modeled using a two-material-layer superlattice. The well layer is GaAs and has a thickness of 24 atomic monolayers, 68 Å, while the barrier layer is $Al_{0.3}Ga_{0.7}As$ and has a thickness of 39 atomic monolayers, 85 Å. The growth direction of the superlattice is the [100] direction, that is, along one of the principal axes of the constituent materials' unit cells, and the material layers are lattice matched so that the superlattice materials are unstrained. These calculations are done for a semiconductor sample at room temperature, although low-temperature cases can also be treated by adjusting the empirical pseudopotential form factors. In the implementation of the formalism, the band-gap discontinuity was split with 43% allotted to the valence-band offset between the materials. The initial coefficients for the wave-packet superposition state were determined by using the fact that these coefficients are proportional to the square root of the interband electron transition rates. The transition rates are normalized to the first heavy-hole to first conduction-band transition rate. The transition rate is then taken as

$$W_n = \frac{I_1(n)}{\hbar\omega_1} \frac{|p_{cv}(n)|^2}{2m} m_r^* n \ , \tag{10}$$

where we have used the two-dimensional density-of-states result in Eq. (9) and constants are normalized to unity. The reduced effective mass m_r^* is used for the two-dimensional mutual density of states and n is the quantum number of the subband state that is used in the wave packet. The use of the two-dimensional density-of-states result is appropriate for the case of an isolated quantum well. Excitonic corrections to the transition rate were not made in this example.

The squared moduli of the envelope functions for the two valence subbands used in forming the wave packet are plotted in Figs. 2(a) and 2(b) for one full subband period. We see that the system being modeled does in fact act as an isolated quantum well. The heavy-hole state is confined within the well and the light-hole state also tunnels only slightly into the barrier layer, before going essentially to zero at the center of the barrier. The HH1 state lies 13.8 meV below the bulk valence-band edge of GaAs, while the LH1 state lies 33.5 meV below

the same point in energy. The subbands are separated by 19.7 meV. This energy separation gives the characteristic time over which any coherent dynamics will occur. An energy separation of 19.7 meV translates into a time constant of 210 fs.

The laser pulse which forms the wave packet couples the first heavy-hole and first light-hole states to the first conduction state. Hence a hole wave packet resulting from interference between the first two valence subbands results in this case. We note that these two hole subbands are easily coupled to only the first conduction subband, $C1$, since the second conduction subband lies approximately 122 meV above the $C1$ subband. Thus there are only two transitions of interest in the formation of the superlattice wave packet. The initial shape of a wave packet formed in this system is illustrated in Fig. 2(c). This wave packet is formed using a Gaussian laser pulse centered at 830.5 nm with a pulse length of 94 fs, full width at the $1/e$ point of the pulse. The light pulse is circularly polarized, that is, it is a linear combination of equal amounts of light linearly polarized normal and parallel to the growth direction. We see that the wave packet looks similar to the subband envelope functions, except that it is slightly sharper and more localized. This slight increase in the localization is a result of the interference of the two subbands included in the wave-packet state. The fact that the wave packet as plotted in Fig. 2(c) is not continuous at the interface between the second and first material layers arises due to round-off error and numerical noise in the calculation. The physical wave packet is, of course, continuous at all boundaries.

The time dependence of the wave packet is illustrated in Fig. 3. In Fig. 3(a), the probability difference between the wave packet at some time after the initial excitation and the initial wave packet is plotted. A negative value of probability difference means that the carriers that make up the wave packet are less likely to be at that point than they were initially. The probability difference is plotted at $\frac{1}{4}$, $\frac{1}{2}$, $\frac{3}{4}$ and one full period of the wave-packet motion. This period is given by the energy separation of the two subbands and is equal to 210 fs. We see that the wave packet shifts to one side of the well and then returns to its initial form after one period. These oscillations will continue with perfect regularity until the wave packet is destroyed. We see this in Fig. 3(b) where the probability difference is plotted at times equal to $\frac{1}{2}$, 1, $\frac{3}{2}$, and 2 periods. Thus, two full periods of the oscillation are plotted but only two lines can be seen. This is because the probability difference is identical at times equal to $\frac{1}{2}$ and $\frac{3}{2}$ of a period and is zero at times equal to one

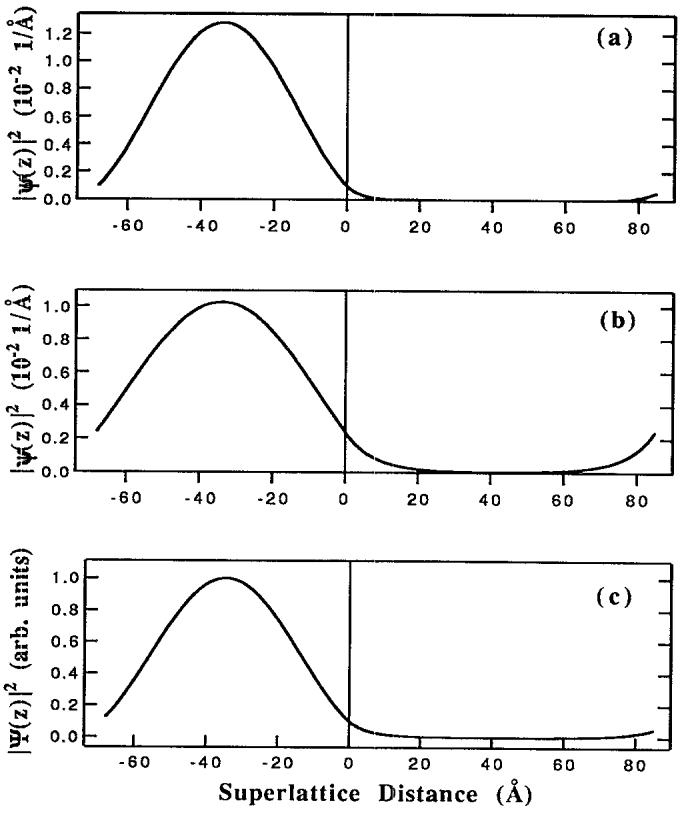

FIG. 2. The squared modulus of the total envelope functions of the two hole states combined to form the wave packet and of a wave packet are plotted for one superlattice period, along the growth direction. Normalization follows the definition of the envelope function. The two states are (a) HH1 and (b) LH1. (c) A wave packet of the system. The exciting laser light is circularly polarized. Negative values of distance lie in the well. Positive values of distance lie in the barrier, with the vertical line marking the interface location. This treatment of the horizontal axis is the same in all figures describing this example.

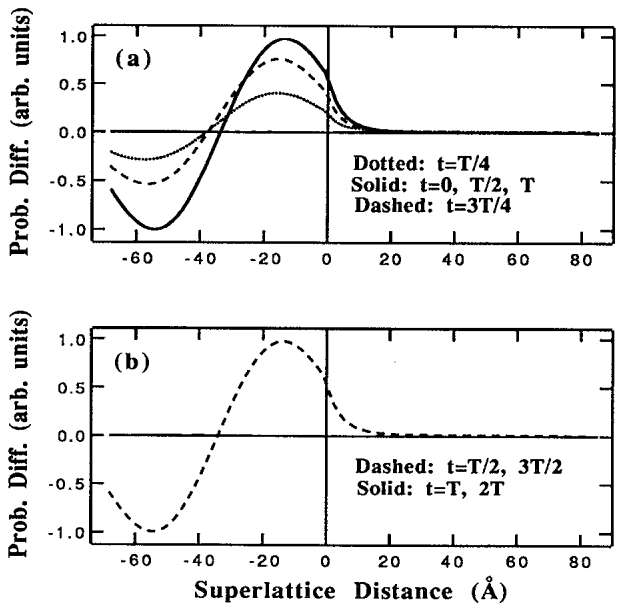

FIG. 3. The difference between the initial wave-packet probability function and the probability function at later times, that is, $\Psi(t)^*\Psi(t)-\Psi(0)^*\Psi(0)$, is plotted to show the time dependence of the wave packet. The period of oscillation is $T=210$ fs. (a) The time dependence over one period shows a shift of the wave packet to one side of the well and then back. (b) Time dependence over two periods shows perfect periodicity of wave-packet dynamics.

and two full periods. We see this behavior because only two subbands are included in this wave packet and so there is only one time constant involved in the total coherent time dependence. This is unlike the Rydberg atomic case in which "higher-order terms" in the time dependence cause more complex dynamics.[2] This wave packet will not break up as long as the coherent dynamics of the system dominate and the simple harmonic time dependence will continue to be manifested. Again, it should be noted that the discontinuity in the probability difference between the second and first material layers arises in the computational process and is not real. The plots in Fig. 3 should be continuous, but round-off error and numerical noise cause the lack of matching at one interface.

IV. THREE- AND FIVE-SUBBAND WAVE PACKETS

Wave packets that are composed of more than two subbands are of interest because they will often arise in physical situations due to real subband energy spacings and the availability of femtosecond laser pulses. The complex coherent dynamics these wave packets exhibit are also of interest. Also, modeling these types of systems serves to display the flexibility of this formalism. We model both three-[25] and five-subband wave packets in coupled-well systems. The number of subbands included in a wave packet is determined directly by the frequency bandwidth and center frequency of the exciting laser pulse. These characteristics of the laser pulse determine which subbands are coupled into the wave packet. All calculations are done using the same input parameters and conditions as in the two-subband wave-packet example unless specifically stated otherwise. Also, all calculations are the same except that the three-dimensional density-of-states result is used. This is appropriate in the case of a series of strongly coupled wells. The unit cell in the coupled-well cases consists of four material layers.

Looking specifically at the three-subband case, the first and third layers are GaAs wells of thickness 9 and 14 atomic monolayers, 25 and 40 Å, respectively. The second and fourth material layers are $Al_{0.3}Ga_{0.7}As$ barriers of thickness 5 atomic monolayers, 14 Å. This unit cell repeats throughout the sample so that the superlattice is, effectively, a series of coupled quantum wells of alternating thicknesses. Only three interband transitions are of interest in the formation of this wave packet. This is because the subband energy levels in the valence and conduction wells are arranged in such a way that the first three hole subbands can be coupled to the first conduction subband alone. Hence this superposition state is given exactly by Eq. (5) and we again have a hole wave packet. The subbands included in the wave packet are the first heavy-hole state, the first light-hole state, and the second heavy-hole state which lie 28.5, 40.3, and 52.7 meV below the GaAs bulk band edge, respectively. This leads to a separation of 11.8 meV between the HH1 and LH1 states and 12.4 meV between the LH1 and HH2 states. Thus there is about a 5% difference in the separations. The LH1 subband lies between the HH1 and HH2 subbands which are split from a single state of an isolated quantum well. The squared modulus of the total envelope functions for the HH1, HH2, and LH2 subbands are plotted for one full superlattice period in Fig. 4.

The wave packets that result from two different laser pulses are modeled. The initial wave packets are shown in Fig. 5. The wave packet of Fig. 5(a) is formed when a Gaussian laser pulse centered at 814 nm, with a pulse length of 66 fs, full width at the $1/e$ point of the pulse, is used. The light is linearly polarized in a direction normal to the growth axis. This wave packet consists of equal contributions from each of the hole states, to within 2%. This wave packet is used in the time-dependent discussion below. The wave packet of Fig. 5(b) is formed when the exciting laser pulse is centered at 810 nm and has full width at the $1/e$ point of the pulse of 77 fs. The polarization is the same. In this superposition, the ratio of the HH1 contribution to the LH1 contribution is 1 to 2 while the HH1 to HH2 ratio is 1 to 3. The relative amount of

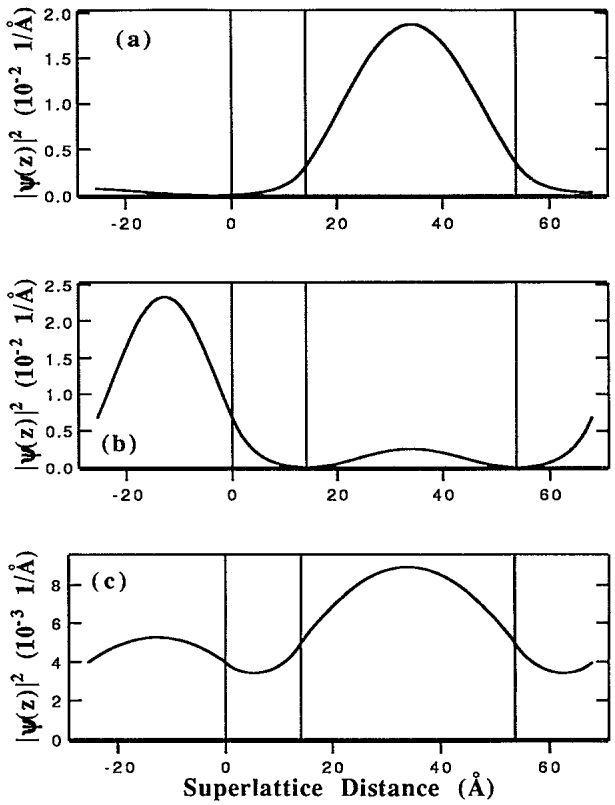

FIG. 4. The squared modulus of the total envelope functions of the three hole states combined to form the wave packet are plotted for one superlattice period, along the growth direction. Normalization follows the definition of the envelope function. The three states are (a) HH1, (b) HH2, and (c) LH1. The vertical lines mark material interfaces. Negative values of the horizontal coordinate are associated with the narrower well and the wider well is the third material layer from the left. The second and fourth material layers from the left are the barrier layers of equal thickness. This description of the distance coordinate is used in all plots describing this example and in the five-subband case.

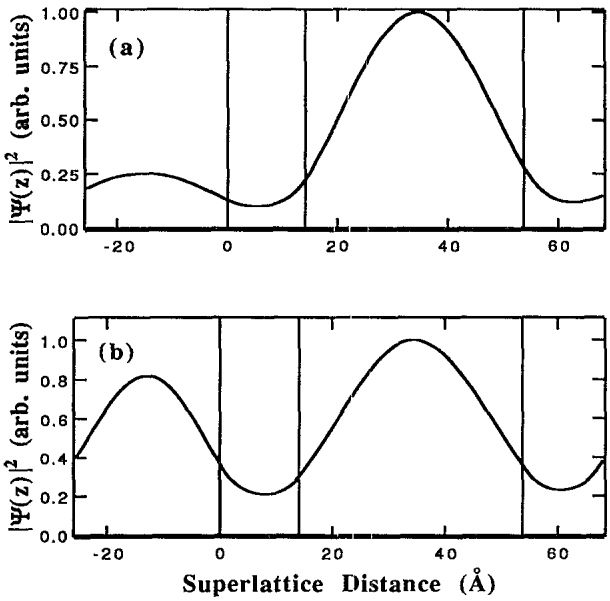

FIG. 5. The squared modulus of the envelope function of the wave packet immediately after excitation is plotted in two cases. (a) Approximately equal amounts of each of the hole subbands contribute to the wave packet. It is well localized in the wider well. (b) Wave packet when the ratio of the HH1 to LH1 contribution and HH1 to HH2 contributions are 1 to 2 and 1 to 3, respectively. The wave packet is more balanced between the wells.

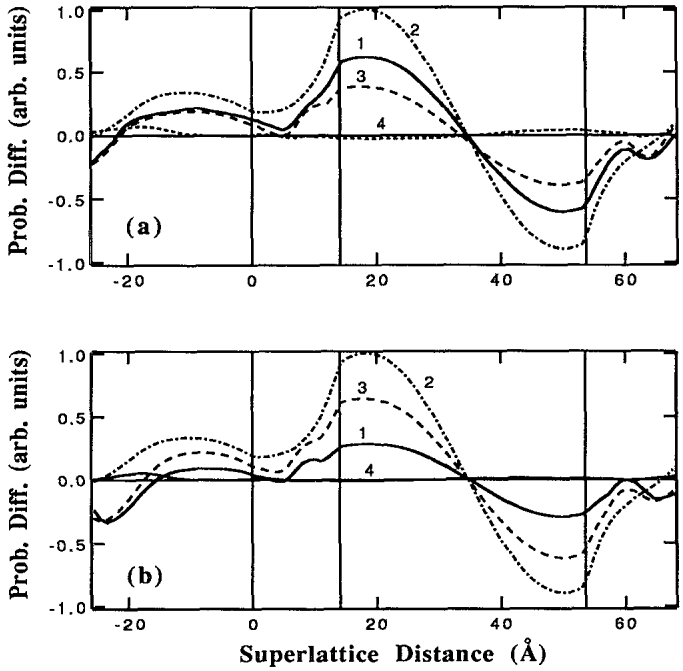

FIG. 6. The difference between the initial wave-packet probability function and the probability function at later times, that is, $\Psi(t)^*\Psi(t)-\Psi(0)^*\Psi(0)$, is plotted for one superlattice period. The wave packet is shown in Fig. 5(a). (a) The wave packet shifts to the left and then back to approximately its initial shape at $t=333$ fs. The times shown are (1) $t=83.5$ fs, (2) $t=166$ fs, (3) $t=249$ fs, and (4) $t=333$ fs. (b) Decay and revival of the wave packet. The results are plotted at multiples of the period, $T=333$ fs. The revival is seen in the fact that the probability difference goes to zero at the final time noted. The times are (1) $t=5$ T, (2) $t=10$ T, (3) $t=15$ T, and (4) $t=20$ T.

the HH2 eigenstate in the wave packet is thus much greater than in the previous case and we see a more balanced wave packet between the two wells. This follows directly from the form of the HH2 envelope function. The dependence of the wave-packet form on the laser pulse is well illustrated in these two cases.

The predicted coherent time dependence of the three-subband wave packet displays a phenomenon previously predicted and seen in atomic systems. This phenomenon is the decay and revival of the wave packet over times long compared to the "period" of the wave-packet motion. In Fig. 6(a) we see that the wave-packet dynamics are quasi periodic, with the wave packet shifting within the wider well and then returning to approximately its initial position after one effective period. The effective period follows from the energy separations between the subbands in the wave packet and is equal to about 333 fs. In Fig. 6(a) the difference between the initial wave packet and the wave packet at a later time is plotted as probability difference. Negative values of probability difference imply that the carriers are less likely to be found at a given point than they were initially.

The time dependence is not perfectly periodic in this case, however. Due to the unequal energy spacings between the hole eigenstates the wave packet breaks up. This is exactly analogous to the breakup of the wave packet seen in atomic systems.[2,15] Atomic systems also show a revival of the wave packet, an effect that results from nonlinear terms occurring in the time dependence of the atomic wave packet. These terms are the direct result of unequal energy spacings between the atomic eigenstates used in the wave packet. The analogy between the atomic and superlattice systems can then be extended because the unequal energy spacings in the superlattice case also lead to a revival of the wave packet. This is seen in Fig. 6(b), where the probability difference between the initial wave packet and the wave packet at a later time is plotted for four different times. Initially, the probability difference is zero across the entire superlattice period because we are comparing the initial wave packet to itself. Looking at times equal to 5, 10, 15, and 20 full "periods" after the excitation, we see that the wave packet does not return to its initial form after 5, 10, and 15 periods, with the greatest deviation coming after 10 periods. However, after 20 periods, the probability difference has almost returned to zero across the entire superlattice. Thus the wave packet has returned to its initial form, that is, it has revived. The time for the revival is consistent with the 5% difference in the subband energy separations. After 20 periods enough "error" has been put into the time dependence that the system returns to its initial form and a revival occurs.

In all cases studied so far, the total modulation of the wave packet has been small. This is why the probability difference has been used in many cases. The modulation can be increased by increasing the interference in the

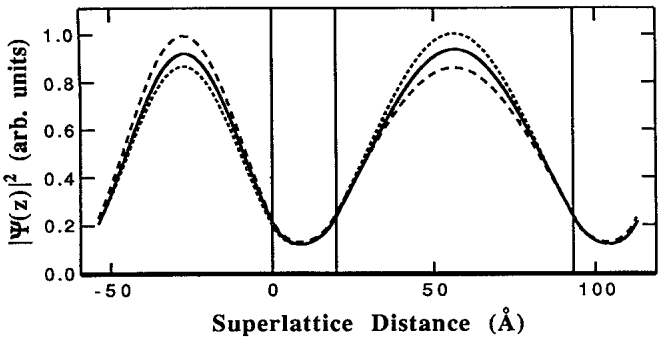

FIG. 7. The squared modulus of the envelope function of the wave packet initially and at two later times is plotted for one superlattice period. The solid line is for $t=0$, the dashed line is for $t=150$ fs, and the dotted line is for $t=450$ fs. The wave packet tends to move into the narrower well and then into the wider well for the times shown.

wave packet. This can be done by including more subbands in the wave packet. An example of this is a five-subband wave packet in a coupled-well system. The superlattice is again modeled using a four-material-layer repeat cycle. The first and third layers are GaAs layers of thickness 19 and 26 atomic monolayers, 54 and 74 Å, respectively. The second and fourth layers are $Al_{0.3}Ga_{0.7}As$ barrier layers of thickness 7 atomic monolayers, 20 Å. We see that the wells are much wider than in the previous case leading to more closely spaced energy levels. Five hole subbands are combined in the wave packet, the heavy-hole 1, 2, and 3 states and the light-hole 1 and 2 states. These states are spread in energy over 40.3 meV and their energy separations vary from 6.3 to 17.7 meV. The coherent time dependence will be quite complex in this case since the energy separations between the five hole states have widely varying values. The largest separation is almost three times larger than the smallest.

A wave packet is produced by coupling the five hole states to a single conduction-band state using a Gaussian laser pulse centered at 835.6 nm and with a pulse length of 132 fs, full width at the $1/e$ point of the pulse. The light is polarized normal to the growth direction. The coherent time dependence of the wave packet is illustrated in Fig. 7, where the initial wave packet and the wave packet at two subsequent times are plotted. Due to the complexity of the time dependence arising from the subband energy level structure, no clearly defined "period" could be found for this time dependence. Although the time dependence is quite complex in this case, we do see that the wave packet deviates fairly substantially from its initial form. The wave packet first tends to move into the narrower well and then reverses itself and is localized more in the wider well. This oscillation between the two wells will continue without a clearly defined period until the wave packet is destroyed by some process such as carrier-carrier scattering. The modulation of the wave packet is approximately $2\frac{1}{2}$ times larger here than in the three-subband case, consistent with fact that more subbands were included in this wave packet.

V. CONCLUSIONS

In conclusion, we have presented a flexible theory which provides a means for describing coherent dynamics in a semiconductor heterostructure excited by a short laser pulse. The theory can describe a wide variety of superlattice and quantum-well systems. It allows for many different III-V and II-VI materials to be used, for various growth directions, for lattice-mismatched induced strain, for applied electric fields, and various other effects. The coherent dynamics are described in a wave-packet formalism which uses the superlattice envelope functions as basis functions in which to expand the wave packet. A number of specific examples were treated. In treating these cases, it was seen that the formalism is consistent with previous experimental and theoretical results in atomic physics.

Additionally, the predictions of the theory are consistent with experimental results in quantum-well systems. For example, organized, periodic dynamics are exhibited only by wave-packet systems with evenly, or nearly evenly, spaced energy levels. This is consistent with an enhanced nonlinear susceptibility being observed only in a quantum-well system in which the eigenstates of interest are approximately equally spaced in energy.[8] Our formalism predicts strong cooperative dynamics when the energy spacings are even. However, more work is required to establish a quantitative relationship between this theory and the results for the third-order nonlinear susceptibility, particularly in light of the fact that the enhanced nonlinear susceptibility is a steady-state effect.

The results of this formalism are particularly interesting when viewed in light of the experimental evidence for wave packets in quantum-well systems. The two-subband wave-packet system modeled here exhibited simple periodic motion with a definite period. This is consistent with the results of both of the wave-packet experiments referred to.[6,7] It should be noted that these wave-packet experiments were conducted in coupled-well systems. We have seen that the theoretical formalism presented here can readily be used to treat coupled-well systems. The five-subband wave packet was predicted to oscillate between the coupled wells. This oscillation between coupled wells leads to the submillimeter-wave emissions of the more recent wave-packet experiment. Also, the periodicity of the three-subband wave packet with its nearly equally spaced energy levels is consistent with what one would project to occur if more than two equally spaced levels were included in a wave packet. Finally, the theory provides insight into possible further work on semiconductor wave-packet systems. The prediction of coherent wave-packet decays and revivals provides a basis for attempting to see this type of behavior in a semiconductor system. Additional experiments can be proposed based on further applications of this formalism to superlattice systems.

ACKNOWLEDGMENTS

The authors would like to acknowledge the assistance of Christian Mailhiot, Gray Wicks, and Ian Walmsley, and the support of the Army Research Office.

*Present address: Physics Department, Whitworth College, Spokane, WA 99251-3901.

[1]John A. Yeazell, Mark Mallalieu, and C. R. Stroud, Jr., Phys. Rev. Lett. **64**, 2007 (1990); G. Alber and P. Zoller, Phys. Rep. **199**, 231 (1991); W. A. Henle, H. Ritsch, and P. Zoller, Phys. Rev. A **36**, 683 (1987); D. Huber, E. J. Heller, and R. G. Littlejohn, J. Chem. Phys. **90**, 7317 (1989).

[2]Z. Dacic Gaeta and C. R. Stroud, Jr., Phys. Rev. A **42**, 6308 (1990); Johnathon Parker and C. R. Stroud, Jr., Phys. Scr. **T12**, 70 (1986).

[3]E. O. Göbel, K. Leo, T. C. Damen, J. Shah, S. Schmitt-Rink, W. Schäfer, J. F. Müller, and K. Köhler, Phys. Rev. Lett. **64**, 1801 (1990).

[4]Mark L. Biermann, Ph.D. thesis, University of Rochester, 1991.

[5]Karl Leo, Theo. C. Damen, Jagdeep Shah, Ernst O. Göbel, and Klaus Köhler, Appl. Phys. Lett. **57**, 19 (1990).

[6]Karl Leo, Jagdeep Shah, Ernst O. Göbel, Theodore C. Damen, Stefan Schmitt-Rink, Wilfried Schafer, and Klaus Köhler, Phys. Rev. Lett. **66**, 201 (1991).

[7]Hartmut G. Roskos, Martin C. Nuss, Jagdeep Shah, Karl Leo, and David A. B. Miller, Phys. Rev. Lett. **68**, 2216 (1992).

[8]Carlo Sirtori, Federico Capasso, Deborah L. Sivco, and Alfred Y. Cho, Phys. Rev. Lett. **68**, 1010 (1992).

[9]J. A. Yeazell and C. R. Stroud, Jr., Acta Phys. Pol. A **78**, 253 (1990).

[10]D. L. Smith and C. Mailhiot, Phys. Rev. B **33**, 8345 (1986).

[11]P. O. Löwdin, J. Chem. Phys. **19**, 1396 (1951).

[12]R. C. Miller, A. C. Gossard, D. A. Kleinman, and O. Munteanu, Phys. Rev. B **29**, 3740 (1984).

[13]Mark L. Biermann and C. R. Stroud, Jr., Appl. Phys. Lett. **58**, 505 (1991).

[14]Jonathan Parker and C. R. Stroud, Jr., Phys. Scr. **T12**, 70 (1986); J. A. Yeazell and C. R. Stroud, Jr., Acta Phys. Pol. A **78**, 253 (1990); J. Parker and C. R. Stroud, Jr., Phys. Rev. Lett. **56**, 716 (1986); G. Alber, H. Ritsch, and P. Zoller, Phys. Rev. A **34**, 1058 (1986); J. A. Yeazell and C. R. Stroud, Jr., *ibid.* **43**, 5153 (1991).

[15]J. A. Yeazell, Mark Mallalieu, and C. R. Stroud, Jr., Phys. Rev. Lett. **64**, 2007 (1990).

[16]J. A. Yeazell and C. R. Stroud, Jr., Phys. Rev. A **35**, 2806 (1987).

[17]B. K. Ridley, *Quantum Processes in Semiconductors* (Clarendon, Oxford, 1988), pp. 184–210.

[18]Claude Weisbuch and Borge Vinter, *Quantum Semiconductor Structures* (Academic, New York, 1991), p. 21.

[19]Claude Weisbuch and Borge Vinter, *Quantum Semiconductor Structures* (Ref. 18), p. 32.

[20]B. K. Ridley, *Quantum Processes in Semiconductors* (Clarendon, Oxford, 1988), p. 61.

[21]W. Z. Lin, G. Fujimoto, E. P. Ippen, and R. A. Logan, Appl. Phys. Lett. **50**, 124 (1987).

[22]F. W. Wise, I. A. Walmsley, and C. L. Tang, Appl. Phys. Lett. **51**, 605 (1987).

[23]Claude Weisbuch and Borge Vinter, *Quantum Semiconductor Structures* (Ref. 18), pp. 108 and 109.

[24]M. J. Rosker, R. W. Wise, and C. L. Tang, Appl. Phys. Lett. **49**, 1726 (1986).

[25]Mark L. Biermann and C. R. Stroud, Jr., Appl. Phys. Lett. **58**, 2279 (1991).